THE TEMPERATURE DEPENDENCE OF THE DYNAMIC AMPLIFICATION FACTOR




J. KALIN
ZAG Ljubljana, Slovenija.
Obtained his B.Sc. from University of Ljubljana

A. ŽNIDARIČ
ZAG Ljubljana, Slovenija.
Obtained his Ph.D. from University of Ljubljana

A. ANŽLIN
ZAG Ljubljana, Slovenija.
Obtained his Ph.D. from University of Ljubljana

D. HEKIČ
ZAG Ljubljana, Slovenija.
Obtained his M.Sc. Eng from University of Ljubljana

Abstract
Bridge Weigh-in-Motion (B-WIM) systems transform the existing bridges or culverts into weighing scales, where the strains measured on the superstructures are used to calculate the axle loads, gross weights, axle spacings and other parameters of the crossing vehicles. The same data can be used for other purposes, including evaluating the dynamic component of bridge traffic loading, the so-called Dynamic Amplification Factor (DAF). An FFT–based method has been recently developed to evaluate DAFs caused by thousands of vehicles crossing the bridges. On some of them, the measurement duration resulted in large ambient and bridge temperature ranges. This paper presents the initial results of the investigation into the possible DAF temperature dependence. Data from two bridges were examined. It was observed that, although the temperature affected both the static and dynamic responses, their ratio remained within the bounds of statistical error. These results indicate that DAF can be regarded as temperature-independent and implies that, when performing bridge structural analyses, there is no need for additional consideration of temperature influences on dynamic allowances.

Keywords: Bridge Weigh-in-Motion, B-WIM, Dynamic Amplification Factor, DAF, Temperature dependence

1. Introduction

The dynamic aspect of vehicle loading on bridge structures is typically considered with a Dynamic Amplification Factor (DAF) – a dimensionless coefficient representing the quotient of the dynamic load-induced effects relative to the static load-induced effects exerted upon a bridge. The European Comission financed ARCHES project (Gonzalez et al., 2009) went into some detail about the dynamic effects of traffic on bridges. It provided an overview of the

current design code recommendations for dynamic allowances and compared those with the simulations and with the measured allowances obtained using Bridge Weigh-in-Motion (B-WIM) (Moses, 1979) measurements on several bridges. One of the more important conclusions was that the design code recommendations are conservative with respect to true dynamic allowance values, especially at higher (extreme) traffic loads. For structural assessment of existing bridges and, in many cases, extending their lifetime, it is thus beneficial to apply more accurate methods of estimating dynamic allowances.

B-WIM systems transform the existing bridges or culverts into weighing scales (Corbally et al., 2014; Moses, 1979). The B-WIM algorithm uses the strains measured on a bridge or culvert superstructure to calculate the axle loads of the crossing vehicles. Traditionally, strains are acquired on the bridge main longitudinal members to provide response records of the structure under the moving vehicle load. However, other locations can be used to improve the results. On slab bridges, the strain sensors are typically mounted equidistantly at the mid-span, across the entire width of the bridge. Measurements during the whole vehicle crossing over the structure provide redundant data, facilitating the evaluation of axle loads.

Knowing that the response of practically any bridge changes with temperature, this manuscript raises a question if DAF itself is temperature-dependant and presents the results of an initial analysis of two DAF datasets derived from a reinforced concrete slab and a composite highway underpass constructed with steel I-girders and a reinforced concrete deck.

2. B-WIM for measurement of the dynamic amplification factor

B-WIM systems are not only used for weighing heavy vehicles. They can, due to their data analysis architecture, provide additional information to support the structural safety analysis (Žnidarič and Kalin, 2020), to develop traffic loading schemes for the structural analysis of existing bridges (Žnidarič, Turk and Kreslin, 2022), and DAF calculations (Kalin et al., 2022).

2.1. The B-WIM theoretical background

The first step in the weighing procedure selects and combines parts of a continuous stream of measured data into the so-called events, which contain signals from one or more vehicles whose influences on the bridge overlap. Axles of vehicles within events are identified, their velocities calculated, and the individual axles joined into vehicles. Finally, the N unknown axle weights A_i in each event are calculated from a system of M equations:

$$g(t_j) = \sum_{i=1}^{N} A_i I\left(v_i(t_j - t_i)\right); \quad j = 1 \dots M, \tag{1}$$

$g(t_j)$ are the bridge responses measured at M different times and $I(x) = I\left(v_i(t_j - t_i)\right)$ is the known influence line at location x. Axle velocities v_i and the arrival times of individual axles t_i determine the location of each axle at the time t_j. The inputs from all strain sensors are used to minimise the influence of the varying transverse positions of vehicles. With the sampling rate of 512 samples per second and a typical vehicle crossing time of a few seconds, the number

of equations is typically two orders of magnitude larger than the number of unknowns. This over-determined system of equations is solved for A_i, in the least-square sense, using the singular value decomposition algorithm (Press et al., 2007).

Influence lines define the response of the bridge at the sensor location to the passage of a unit axle load. They are the critical structural parameters that directly affect the B-WIM measurement quality. For the last 20 years, B-WIM systems have used influence lines derived directly from the measured data on the site (Žnidarič and Lavrič, 2010; Žnidarič et al., 2010). The latest influence line calculation method developed at the Slovenian National Building and Civil Engineering Institute (ZAG) uses equation (1), in which the function $I(\mathrm{x})$ is also unknown and is calculated using Powell's minimisation technique (Press et al., 2007). The possibility of calculating actual influence lines is exceptionally beneficial in analysing the existing bridges (Žnidarič and Kalin, 2020). The influence line calculation procedure details are given in Žnidarič et al. (2017).

Figure 1 presents an example of weighing a 40.5 t four-axle tractor-trailer crossing a 10.5 m integral concrete slab bridge at 50 km/h. The red trace is the sum of measured signals, the black spikes are the positions of the four axles, the green traces are the influence lines at axle positions multiplied by raw axle loads, and the blue trace is the sum of these axle contributions.

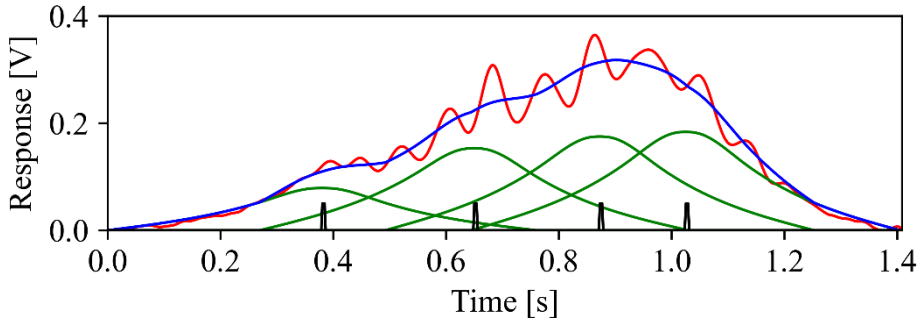

Figure 1 - An example of the B-WIM weighing result

2.2. Measuring DAF with B-WIM

Several dynamic amplification definitions exist, describing the increase of the static load due to the presence of dynamic components (Gonzalez et al., 2009). This paper defines DAF as:

$$DAF = \frac{y_T}{y_S} \tag{2}$$

where y_T is the maximum total (static + dynamic) load effect due to a particular loading event and $y_S$is the maximum static load effect for the same loading event. With this definition, the maxima of total and static load effects need not coincide.

The total load effect is readily available – it is simply the measured bridge response to a vehicle passage. However, the static load effect must be estimated from the total load effect. This

paper's method assumes that the load effect's static and dynamic components can be separated based on their characteristic frequencies (Gonzalez et al., 2009). The characteristic frequency of the dynamic component is assumed to be higher than the frequencies present in the static component. The signal is transformed into the frequency domain using the Fast Fourier Transform (Press et al., 2007), the spectrum low-pass filtered at a certain pre-determined cut-off frequency and transformed back into the time domain. The remaining is taken as the static load effect and is used in calculating the DAF value.

As proposed in the ARCHES project (Gonzales & Žnidarič, 2009), the method used to estimate the static component uses FFT filtering to separate the measured signal into static and dynamic components. The latest method evaluates the data twice to avoid the subjective determination of the low-pass filter cut-off frequency (Kalin et al., 2015). In the first pass, each event's cut-off frequency is determined by comparing the low-pass filtered signal with the theoretical signal, determined by the sum of influence lines multiplied by axle loads – the blue trace in Figure 1. Once the complete dataset has been processed, the mean cut-off frequency is used to filter the dataset again, using the low-pass filtered signal as the static signal approximation for the calculation of the DAF.

3. Temperature dependence of DAF

The DAF definition from (2) yields two possible causes of its temperature dependence, the changes in static and dynamic responses. At least for relatively simple concrete bridge structural systems, the static response is expected to increase with temperature since Young's modulus is known to decrease with temperature. Thus, the same stress (traffic loading) causes an increase in strains. Different authors cite factors at around 0.3 %/°C to 0.6 %/°C (Yubo et al., 2014). This paper attempts to answer whether the dynamic component increases in step with the static component, keeping the DAFs the same, or changes more or less than the static component, leading to an increase or decrease of DAFs.

Analysing the dynamic component requires to define y_D, the maximum of the dynamic component. It is obtained by subtracting the static component from the measured signal:

$$y_D(t_i) = y_T(t_i) - y_S(t_i) \tag{3}$$

Note that due to the nonlinearity of the "maximum" operator, in general, $y_D \neq y_T - y_S$.

3.1. Bridge selection and calculations

Two of the 15 bridges analysed by Kalin et al. (2021) were chosen for initial temperature dependence analysis. Bridge A is a single-span 6.0 m long reinforced concrete slab highway underpass located on a Slovenian motorway, with over 720,000 data points collected during 15 months of operation. The temperature variation of 32 °C, measured with a thermocouple inserted into a few centimetres deep hole in the concrete beam, was the highest among the considered bridges. To compare the results with a steel bridge, Bridge B is a single-span 25.0 m long highway composite underpass, a typical US highway structure. It comprises six 1.8 m high

steel I-girders and a reinforced concrete deck. The temperature variance during measurements was 20 °C, measured with a thermocouple glued to a steel girder.

Figure 2 – Side view and view from below of Bridge A

Figure 3 – Side view and view from below of Bridge B

A significant difference between the two sites, apart from structural types and dimensions, was that pavement before and on Bridge A was smooth, while before Bridge B, it was heavily damaged, with uneven surface, potholes and loose asphalt.

The data from both bridges were processed using a two-pass procedure. Table 1 summarises the results. The first two columns in the table are the bridge designation and the number of vehicles considered. DAF and σ_{DAF} are the mean measured DAF and the standard deviation, respectively. T_{min} and T_{max} are the minimum and maximum temperature values for the considered vehicles.

Table 1 – Summary of results

Site	N	DAF	σ_{DAF}	T_{min} [°C]	T_{max} [°C]	k_{DAF} [%/°C]	k_S [%/°C]	k_D [%/°C]	Δ_{DAF}	$\frac{\Delta_{\mathrm{DAF}}}{\sigma_{\mathrm{DAF}}}$
A	724,362	1.09	0.04	-2.2	30.7	-0.011	0.64	0.57	-0.0038	-0.09
B	27,847	1.18	0.15	16.2	36.1	-0.145	-1.96	-2.58	-0.0340	-0.23

A straightforward linear regression dependence model in a form of a of DAF vs T was applied. The following three columns display the slope coefficients for DAF, and the static and the dynamic components, respectively. The units are per cent change per °C.

Looking at k_s, the value 0.64 %/°C for Bridge A (concrete slab bridge) corresponds well with the values from the literature, 0.3 – 0.6 %/°C. The load effect increase is consistent with the expected change of Young's modulus. On the other hand, the correlation for Bridge B is higher and negative, meaning that the bridge stiffens with the rising temperature. Such performance has been observed on some other older steel bridges with non-ideally performing bearings and expansion joints. Yet, discussion about possible causes of such unpredicted behaviour of Bridge B exceeds the scope of this paper.

More importantly, the value of k_D, i.e., the relative dependence of the dynamic component, has the same sign and approximate value as the relative dependence of the static component. This value describes a minimal relative change of DAF with temperature. Factor k_{DAF} is as low as -0.011 %/°C for Bridge A and substantially higher -0.145 %/°C for Bridge B.

To gain some insight into these numbers, it is useful to consider the change of DAF over the whole measured temperature range. The column Δ_{DAF} in Table 1 displays $k_{\mathrm{DAF}}(T_{max} - T_{min})$, the total change of DAF over the entire measured temperature range. In the column $\frac{\Delta_{\mathrm{DAF}}}{\sigma_{\mathrm{DAF}}}$, this value is compared to the standard deviation of DAF, which indicates the statistical importance of the measured temperature dependence.

Figures 4 and 5 present the results. Firstly, each dot present the individual calculated DAF values on both bridges as a function of measured temperature. On the top, the DAF changes with temperature are plotted as linear regression curves with slope coefficient k. The value for Bridge A is hardly noticeable, reaching just -0.09 or -9% of its standard deviation σ_{DAF} (Figure 4). This value is higher for Bridge B (Figure 5), -0.23 or -23%, which is still less than a quarter of the standard deviation and can also be perceived as insignificant. Figure 5 presents the results for Bridge B in its entire DAF ordinate range (left), and for a more straightforward comparison, with the same scale as Bridge A (right).

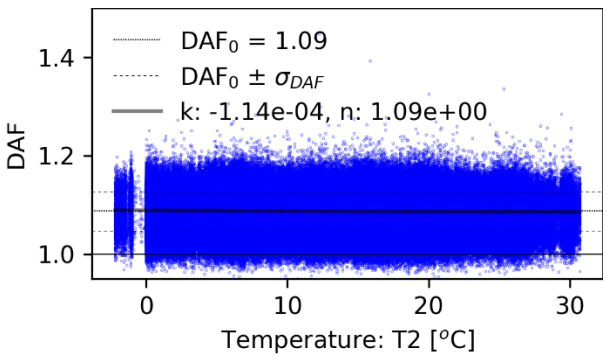

Figure 4 – DAF vs. temperature for Bridge A

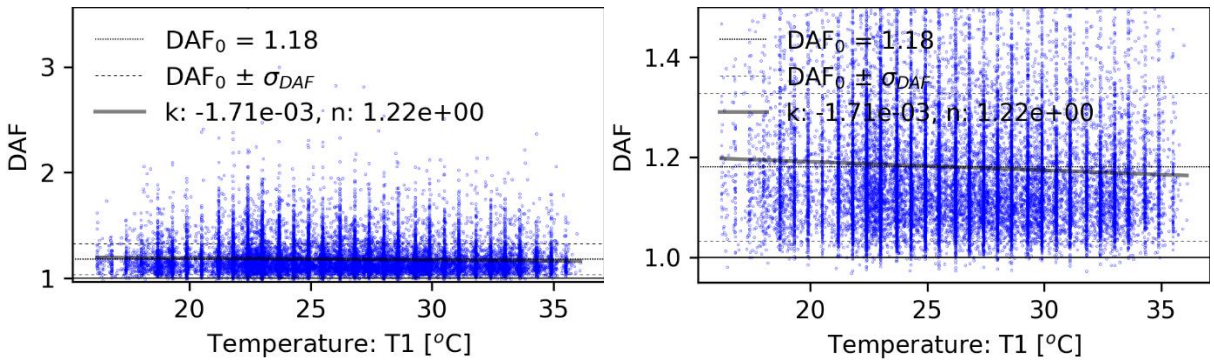

Figure 5 –DAF vs. temperature for Bridge B; the entire DAF range (left), and equal range as in Figure 4 (right)

The dotted lines present the mean, and the dashed lines represent the mean ± one standard deviation of DAF values from both sites. The thick grey lines are the fitted linear functions that barely deviate from the mean DAF and are well within the standard deviation bounds. This yields the conclusion that, on these two bridges, DAF does not depend on temperature.

4. Conclusion

The temperature dependence of DAF has been investigated using B-WIM datasets measured on two structurally dissimilar bridges: a 6-m long concrete slab underpass and a 25-long composite bridge composed of steel I-girders connected by a concrete deck. Dynamic bridge excitations caused by all relevant heavy gross vehicle loading events were calculated with the ZAG's DAF method.

The analysis revealed that the temperature dependence of the static load effect component for the concrete Bridge A aligns well with the anticipated decrease of bridge stiffness as the temperature changes. Conversely, the composite Bridge B displayed an unexpected stiffening effect with rising temperature, which needs further investigation. Nevertheless, in both cases, the variation of the dynamic part of the load effect closely followed the static one, resulting in an insignificant change of DAF with temperature.

The findings suggest that, at least for bridges of similar structural design, temperature seems to affect the DAF negligibly and, therefore, no additional temperature consideration are needed even in detailed structural analyses and safety evaluations. However, the results were analysed for two bridges only, and therefore, the conclusions should be interpreted cautiously. Future studies will include DAF results from more bridges and should incorporate numerical simulations and different damage scenarios to bolster the robustness of these findings.

5. Acknowledgement

The authors would like to express their gratitude for the support from the Slovenian Research Agency programme P2-0273 Building Structures and Materials.

6. References

- Corbally, R., Žnidarič, A., Cantero, D., Haijalizadeh, D., Leahy, C., Kalin, J. & Kreslin, (2014). Algorithms for Improved Accuracy of Static Bridge-WIM Systems: BridgeMon D3.1 report, European Commission.
- Gonzalez, A. & Žnidarič, A. (2009). Recommendations on dynamic amplification allowance: ARCHES deliverable D10, 75, European Commission.
- Moses, F. (1979). Weigh-in-motion system using instrumented bridges. Journal of Transportation Engineering, 105(3), 233–249.
- Kalin, J., Žnidarič, A., & Kreslin, M. (2015). Using weigh-in-motion data to determine bridge dynamic amplification factor. EVACES'15, 6th International Conference on Experimental Vibration Analysis for Civil Engineering Structures. doi: 10.1051/matecconf/20152402003.
- Kalin, J., Žnidarič, A., Anžlin, A., & Kreslin, M. (2022), Measurements of bridge dynamic amplification factor using bridge weigh-in-motion data, Structure and Infrastructure Engineering, 18-8, doi: 10.1080/15732479.2021.1887291.
- Press, W. H., Teukolsky, S. A., Vetterling, W. T., & Flannery, B. P. (2007). Numerical Recipes: The Art of Scientific Computing, 3rd ed,. Cambridge University Press.
- Žnidarič, A., & Lavrič, I. (2010). Applications of B-WIM technology to bridge assessment (pp. 1001–1008). Philadelphia, PA: Proceedings of IABMAS 2010 Conference.
- Žnidarič, A., Kalin, J., & Kreslin, M. (2017). Improved accuracy and robustness of bridge weigh-in-motion systems. Structure and Infrastructure Engineering, 14(4), 412-424, doi: doi.org/10.1080/15732479.2017.1406958.
- Žnidarič, A. & Kalin, J. (2020). Using Bridge Weigh-in-Motion Systems to Monitor Single-Span Bridge Influence Lines. Journal of Civil Structural Health Monitoring. Springer, doi: doi.org/10.1007/s13349-020-00407-2.
- Žnidarič, A., Turk, G. and Kreslin, M. (2022). Determination of characteristic internal forces and moments in road bridges from weigh-in-motion data. Gradbeni vestnik, pp. 82–94. In Slovene.
- Yubo, J., Hanbing, L., Xianqiang, W., Yuwei, Z., Guobao, L., & Yafeng, G. (2014). Temperature Effect on Mechanical Properties and Damage Identification of Concrete Structure, Advances in Materials Science and Engineering, doi: https://doi.org/10.1155/2014/191360.